

Macrophage-mediated biodegradation of poly(DL-lactide-co-glycolide) *in vitro*

Zhidao Xia,^{1,2} Yizhong Huang,³ Iannis E. Adamopoulos,¹ Andrew Walpole,³ James T. Triffitt,¹ Zhanfeng Cui²

¹Nuffield Department of Orthopaedic Surgery, The Botnar Research Centre, Institute of Musculoskeletal Sciences, University of Oxford, Oxford, United Kingdom

²Department of Engineering Sciences, The University of Oxford, Oxford, United Kingdom

³The Department of Materials, The University of Oxford, Oxford, United Kingdom

Received 16 November 2005; revised 10 March 2006; accepted 22 March 2006

Published online 30 June 2006 in Wiley InterScience (www.interscience.wiley.com). DOI: 10.1002/jbm.a.30853

Abstract: Biodegradation of poly-DL-lactide-co-glycolide (PLGA) both *in vitro* and *in vivo* has been well documented. However, the roles that macrophages and their fused multinucleated giant cells (MNGCs) play in this biodegradation are still unclear. The current study aimed to investigate macrophage-mediated biodegradation of PLGA thin films and of PLGA composites with hydroxyapatite (HA) and tricalcium phosphate (TCP) ceramic powders *in vitro* using a murine macrophage cell line (RAW 264.7). The interactions were analyzed by using cell viability assays, scanning electron microscopy, and focused ion beam microscopy. The results showed that RAW 264.7 cells effectively attached and proliferated on the

PLGA films and PLGA-HA, PLGA-TCP composites. The RAW 264.7 cells were observed to aggregate and fuse to form MNGCs. The cell processes on the membrane, or pseudopodia, penetrated into the PLGA films and evidently eroded the surface. We conclude that macrophages and fused MNGCs actively respond to PLGA films as substratum and degrade the surface of this polymer. © 2006 Wiley Periodicals, Inc. *J Biomed Mater Res* 79A: 582–590, 2006

Key words: macrophage; multinucleated giant cells (MNGCs); poly-DL-lactide-co-glycolide (PLGA); biodegradation; focused ion beam (FIB) microscopy

INTRODUCTION

Biodegradable polymers have enormous benefits for use in many short-term medical applications, as these materials can completely and safely degrade and be absorbed by the body after they fulfill their functions.¹ The advantages of degradable polymers have paved the way for a number of sophisticated biomedical applications. Poly-DL-lactide-co-glycolide (PLGA) is one of the approved biodegradable polymers, which have been used for surgical sutures,² drug delivery systems,^{3,4} orthopedic fixing devices,⁵ and tissue engineering scaffolds.⁶

Degradable polymers were classified into two distinct modes of degradation, surface eroding and bulk eroding ones.^{1,7,8} Surface erosion polymers lose material from the surface only. They get smaller but keep their original geometric shape.^{8,9} In bulk ero-

sion, degradation is not confined to the surface of the polymer. Therefore, the size of a polymer device will remain constant for a considerable portion of time.^{8,9} In the case of PLGA degradation, the interior of the polymer is degraded first and disappears over a period of time, and the outer surface remains as a shell and is degraded later.¹⁰

It is generally accepted that, as an aliphatic polyester, the biodegradation of PLGA occurs by bulk erosion.^{8,11} The polymer chains are cleaved by hydrolysis to form monomeric acids and are eliminated from the body as carbon dioxide and water. The rate of hydrolysis of the polymer chain is dependent on significant changes in temperature and pH or the presence of catalyst, and little difference is observed in the rate of degradation at different sites *in vivo*.^{1,11} Enzymatic involvement in the biodegradation of the PLGA has been somewhat controversial.¹¹ However, it has been shown that 50:50 PLGA degraded significantly faster *in vivo* in comparison with the degradation *in vitro*.¹²

It has long been recognized that macrophages can effectively respond to biomaterial implantation and engulf various biomaterial particles.¹¹ Macrophages also participate in extracellular biodegradation of

Correspondence to: Prof. Z Cui; e-mail: zhanfeng.cui@eng.ox.ac.uk

Contract grant sponsors: The Wellcome Trust and EPSRC

extracellular matrices such as collagen by release of a spectrum of enzymes.¹³ Osteoclasts, which differentiate from cells of the monocyte/macrophage lineage, form an acidic environment on mineral surfaces by release of protons, which leads to bone resorption.^{14,15} Foreign body giant cells (FBGCs), another distinct cell population derived from monocytes/macrophages, actively respond to any foreign implants as long as the materials remain *in vivo*.¹⁵

The degradative activity of these cells has resulted in wide interest and concern for their interactivity with all biomaterials. On the one hand, techniques have been developed to eliminate these cells using antibodies or chemicals to reduce the inflammatory responses to implants.¹⁶ On the other hand, the role of these cells in biomaterial degradation and the consequent effects of these cells on tissue regeneration have been intensely studied.^{17–20}

The macrophage is the major differentiated cell of the mononuclear phagocyte system. It originates from bone marrow precursors, which differentiate into peripheral blood monocytes, and macrophages are widely distributed throughout the body.¹³ Macrophages are the dominant infiltrating cells that respond rapidly to biomaterial implantation in soft and hard tissues.^{19,21,22} As a morphologic variant, macrophages can fuse into multinucleated giant cells (MNGC), also called FBGC, and both cell types are observed at the tissue–material interface of medical devices¹⁵ and on implanted tissue engineering scaffolds.²³

MNGC formation results from fusion of mononuclear phagocytes. Both experimental and circumstantial evidence suggests that fusion takes place following the attachment of more than one macrophage to the same endocytic material.²⁴ In addition, FBGCs have been implicated in the biodegradation of polymeric medical devices.²²

Cell–material interactions occur mainly in the interfaces between cells and biomaterials. However, the biological and biochemical processes occurring at the cell–material interface are still very poorly understood. There are several difficulties for detailed study of the cell–material interface. First, for example, osteoclastic cells normally form a low pH microenvironment at the location of biodegradation in an area sealed by a clear-zone. This compartmentalization may have no significant effect on the pH or ion concentration in the remainder of the environment. Second, although the chemical structures of biomaterials are distinguishable from the cellular structures, the essential components of degradation of biomaterials may only be distinguished by specific analytical methods. The transmembrane mass exchanges that occur between the cytoplasm and biomaterial surfaces are thus very difficult to monitor. Finally, the interfacial reactions between cell membrane and materials are on the nanometer scale, and require highly sophisticated techniques to monitor fully.

In other areas of research, interfacial structures have been investigated by preparing samples with a focused ion beam (FIB) system. For example, FIB has been well established as a means of selectively milling to reveal structural features in integrated circuits. In the semiconductor industry, it has been developed as an important tool in defect analysis and circuit modification²⁵ and has been used in transmission electron microscope sample preparation²⁶ and in dental research.²⁷ One of the advantages of the technique is that additional sample preparation is normally not required.

The aim of this study is to observe the biodegradation of PLGA polymer materials *in vitro* by a murine macrophagic cell line, RAW 264.7 using a scanning electron microscope (SEM) and a FIB system. The results clearly indicate that macrophages and their fused MNGCs respond to the polymeric materials and erode PLGA from the surface.

MATERIALS AND METHODS

Materials

α MEM, trypsin-EDTA, penicillin/streptomycin were purchased from Invitrogen, Paisley, UK. Ca^{2+} - Mg^{2+} -free PBS was from Cambrex Bio Science Wokingham, Berkshire, UK. Tissue culture flasks and multiwell plates were from Cellstar[®], Greiner Bio-One, Gloucestershire, UK. Fetal bovine serum (FBS) was purchased from M. B. Meldrum, Bucks, UK. LIVE/DEAD staining kit (contains calcein and ethidium homodimer-1) was from Molecular Probes, Leiden, Netherlands. Receptor activator of nuclear factor kappa B ligand (RANKL) was obtained from Peprotech Europe, Oxfordshire, UK. PLGA was obtained from Boehringer Ingelheim Pharma, Ingelheim, Germany. Hydroxyapatite (HA) and tricalcium phosphate (TCP) ceramic powders were kindly supplied by Plasma Biotol Limited, North Derbyshire, UK. All other materials and chemicals were obtained from Sigma–Aldrich Chemical Company, Dorset, UK.

Fabrication of polymeric and composite thin films

Flat polymeric films were cast on glass coverslips, or on 12-mm diameter titanium discs to increase the strength of support and to diminish electrical charging under electron microscopy. PLGA was dissolved in acetone at 2 g/10 mL (w/v). For making composites, HA or TCP ceramic particles were added into PLGA at a ratio of PLGA:HA (or

TABLE I
The Ratio of PLGA, HA, and TCP in the Solvent for Casting Film

	PLGA (g)	HA (g)	TCP (g)	Acetone (mL)
PLGA	2	–	–	10
PLGA-HA	2	0.5	–	10
PLGA-TCP	2	–	0.5	10

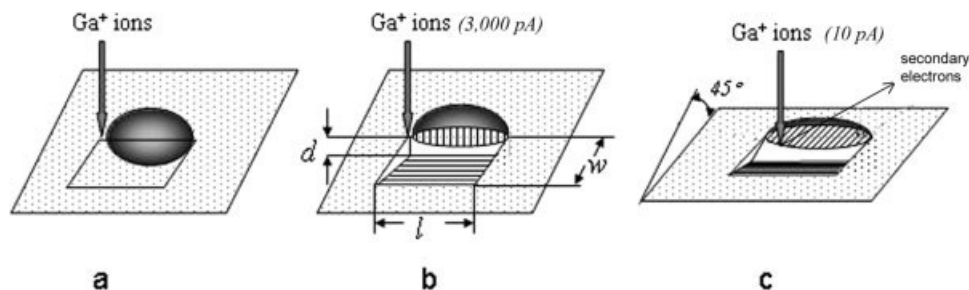


Figure 1. A schematic diagram showing the procedure of cross-sectioning of the sample from its surface by a FIB system: (a) A target cell is selected using a staircase pattern that covers a desired surface; (b) The ion beam with a beam current of 3000 pA etches the selected area ($l \mu\text{m} \times w \mu\text{m}$) until a depth d is achieved; (c) The image for each slice is revealed and recorded at a sample tilt of 45° , in which a beam current of 10 pA is used to minimize the specimen damage during the ion beam scanning.

TCP) = 80:20 (Table I). Fifty microliters of PLGA, PLGA-HA, or PLGA-TCP were directly added onto 12-mm diameter glass coverslips or titanium discs, left in a flow cabinet for 48 h for complete evaporation of solvent, washed twice in PBS for 1 h periods, and incubated in α MEM for 24 h to remove any residual solvent before cell culture.

Cell culture

The RAW 264.7 murine macrophage cell line was recovered from stock in liquid nitrogen,²⁸ and cultured in 10% FBS in α MEM at a seeding density of 4×10^5 cells/cm². The cells were fed using 10% FBS α MEM supplement with 10 ng/mL RANKL to induce osteoclast differentiation. The culture medium was replaced every 3 days.

Samples were harvested at day 1 and day 7 after seeding, washed with PBS twice, and then were used either for LIVE/DEAD staining or fixed by 4% glutaraldehyde (0.1M phosphate buffer solution, pH 7.2–7.4) for microscopy.

Live/dead cell viability assay

At the end of day 1 and day 7, cells were washed twice in PBS to remove any serum derived from the culture medium to assess the cell viability of RAW 264.7 cells on the biomaterials. Samples were stained using a LIVE/DEAD stain kit (Molecular Probes). The kit contains two fluorescent dyes: calcein to stain living cells green and ethidium homodimer-1 (Ethd-1) to stain damaged or dead cells red. Samples were stained using 4 μM calcein and 2 μM Ethd-1 (final concentration) in PBS for 30 min at $(37 \pm 1)^\circ\text{C}$. Samples were rinsed twice using PBS to remove any dye and fixed either in 4% formaldehyde (Sigma–Aldrich) or 4% glutaraldehyde (Sigma–Aldrich) in 0.1M PBS at $(4 \pm 1)^\circ\text{C}$ to prevent cell detachment from the surfaces. Samples were washed again in PBS to remove the fixative before being observed by using fluorescence microscopy. Images were captured using a color video camera (JVC 3-CCD, KY-F55B, Yokohama, Japan) at $100\times$ magnification.

For each sample, three images were captured. Images were opened in Adobe photoshop 6.0 (San Jose, CA) and each image, calibrated as 1.18 mm^2 , was divided into 50 squares using a grid. Live and dead cells were counted in

five squares to estimate the cell numbers in an image. Three indices were selected for analysis as shown in Eqs. (1)–(3).

$$\text{Cells}/\text{mm}^2 = \left(\sum_{i=1}^3 n/3 \right) / C \quad (1)$$

where n is the cell number/image and C is the calibrated area of an image at given magnification.

$$\text{Total cells}/\text{mm}^2 = \text{live cells (green)} + \text{dead cells (red)} \quad (2)$$

$$\text{Viability (\%)} = \frac{\text{average live cells (green)}}{\text{total cell numbers (red + green)}} \times 100\% \quad (3)$$

Scanning electron microscopy

After cell counting by fluorescence microscopy, the cell-biomaterial constructs were fixed in 4% glutaraldehyde, 0.1M PBS for at least 24 h, washed twice in PBS for 5 min, serially dehydrated in 40, 70, 80, 90, 95, and 100% ethanol each for 15 min, infiltrated in 50% hexamethyldisilazane in absolute ethanol and 100% hexamethyldisilazane for 30 min, and washed with fresh 100% hexamethyldisilazane before leaving the samples in a fume cabinet overnight to dry. The dried samples were carbon coated for SEM.

For demonstration of the erosion on the polymeric surfaces, three samples from each group washed in PBS and placed in 10% Triton X100 for at least 48 h to detach any cells and cell fragments. Samples were washed in distilled water to remove the Triton X100 and air dried, and carbon coated for SEM.

FIB microscopy

For FIB microscopy, the cell-biomaterial constructs were fixed in 4% glutaraldehyde, 0.1M PBS (pH 7.2) at 4°C for at least 24 h. To avoid changes of the material surface from dehydration in ethanol, or reaction with other organic solvent, samples were washed in distilled water to remove glutaraldehyde and then mounted onto stubs after being dried in air for 10 min. Before the sample was placed into the FIB system, the sample was coated with a thin layer of gold to minimize charging and consequent damage to the cells.

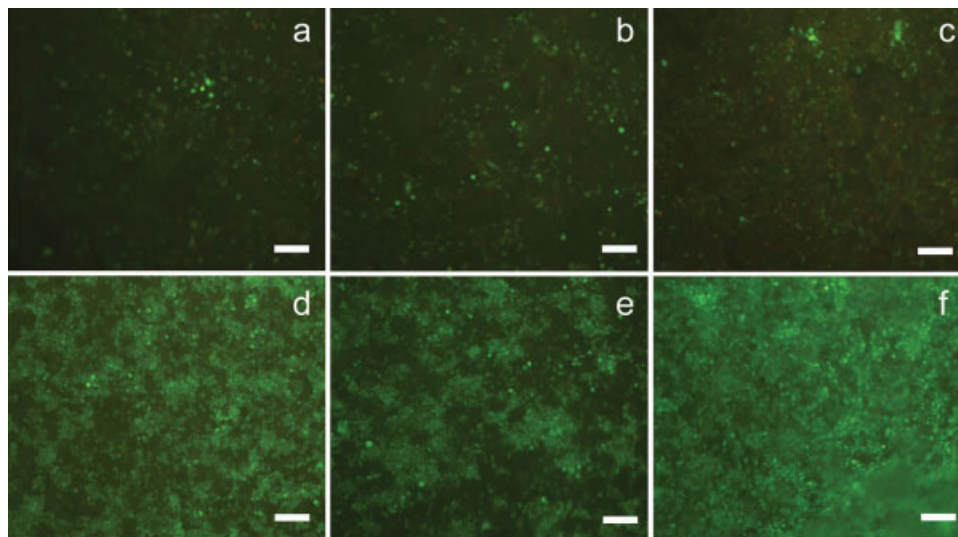


Figure 2. Micrographs of live/dead staining of RAW 264.7 cells on PLGA, PLGA-HA, and PLGA-TCP films. Day 1 after cells were seeded on (a) PLGA, (b) PLGA-HA, and (c) PLGA-TCP. Day 7 after cells were seeded on (d) PLGA, (e) PLGA-HA, (f) PLGA-TCP. Most cells were stained green (live), very few cells were stained red (dead). Bar = 0.1 mm. [Color figure can be viewed in the online issue, which is available at www.interscience.wiley.com.]

The FIB system used for this study was a FEI 200 (FEI UK, Cambridge, UK) which provides a Ga^+ ion beam with the ion energy of up to 30 keV. The ion beam enables material to be removed from the sample surface at specific positions so that cross-sections can be obtained. The system forms secondary electron images and allows viewing of the sample during milling. Hence, the technique can be used for observation of the interface between the cell and the substratum across the interface. The process is schematically illustrated in Figure 1.

Statistics

GraphPad InStat[®] Version 3.06, 32 bit for Windows were used for statistical analysis. Ordinary ANOVA were performed using standard (parametric) methods for Student-Newman-Keuls multiple comparison test. $p < 0.05$ was chosen as significant.

RESULTS

Cytotoxicity assay of RAW 264.7 cells on PLGA, PLGA-HA, and PLGA-TCP

After LIVE/DEAD staining, cell morphology of the RAW 264.7 cells is shown in Figure 2. Quantitative analysis of viability and total cell numbers of RAW 264.7 cells on PLGA, PLGA-HA, and PLGA-TCP films at days 1 and 7 are shown in Figure 3. There were no significant differences of cell viability between the three materials studied at day 1 or day 7. Also, there were no significant differences in total cell number achieved between the three materials at day 1. At day 7, however, it was observed that the total cell

numbers of RAW 264.7 cells on the three materials were significantly higher than those at day1 ($p < 0.001$). The total number of cells on the PLGA-TCP compos-

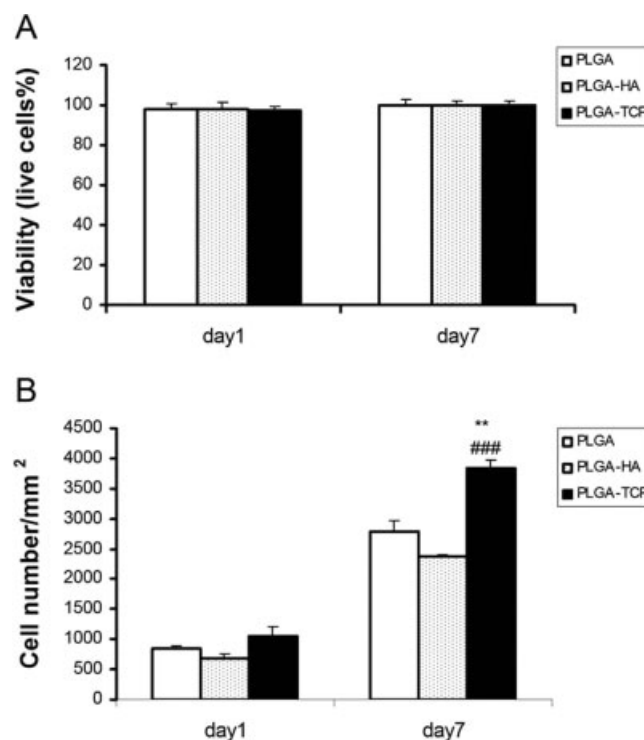


Figure 3. Quantitative analysis of viability and total cell numbers of RAW 264.7 cells on PLGA, PLGA-HA, and PLGA-TCP films at days 1 and 7. (A) viability assay (% live cells) showed no differences between three materials. (B) total cell numbers on three materials. **, compared with the same materials at day 1, $p < 0.001$. ###, compared with PLGA and PLGA-HA, $p < 0.001$.

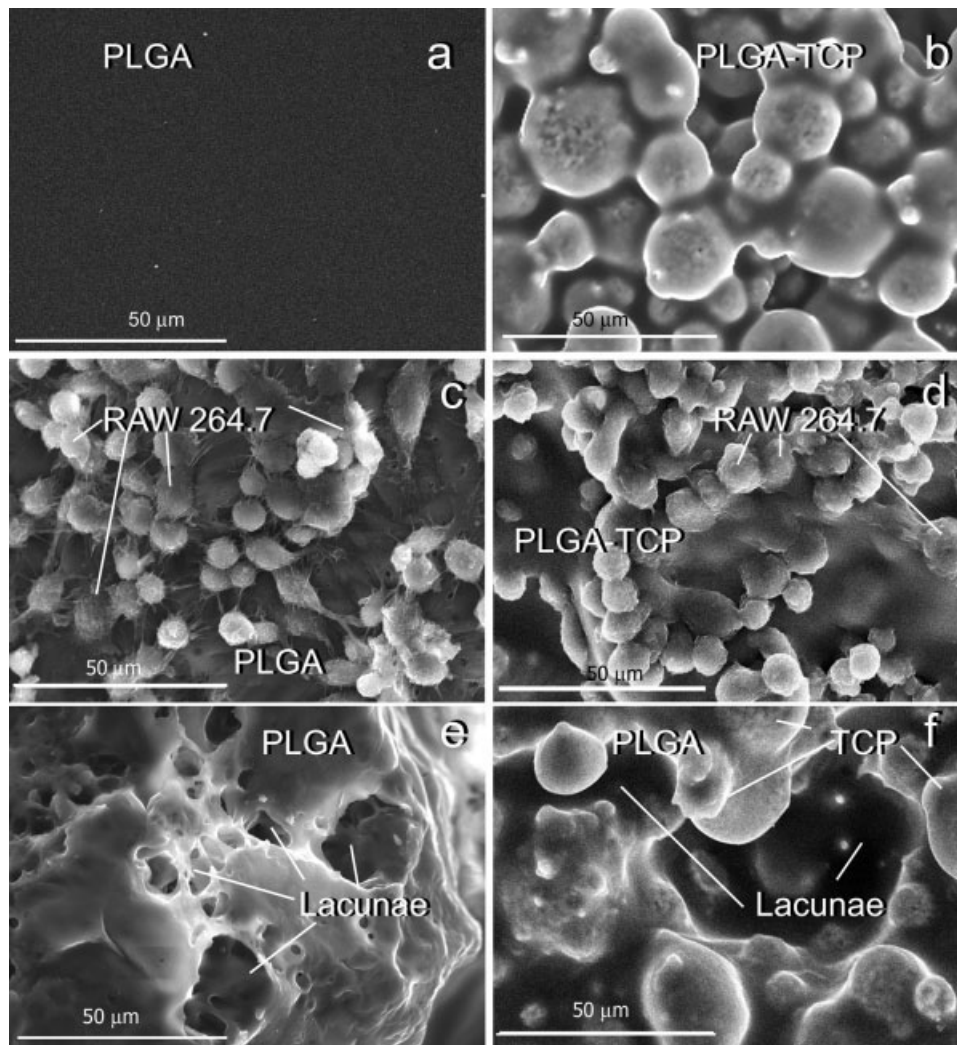


Figure 4. Images of RAW 264.7 cells on PLGA (a, c, and e) and PLGA-TCP composite (b, d, and f) films by SEM. (a) The surface of PLGA film. (b) The surface of PLGA-TCP composite. TCP ceramic particles were evenly coated with a thin layer of PLGA film. (c) 7 days of RAW 264.7 cells on PLGA. (d) 7 days of RAW 264.7 cells on PLGA-TCP. The morphology and sizes of cells were similar to those on the surface of PLGA. (e) By removing cells on PLGA using Triton X100, the surface erosion of PLGA by RAW 264.7 cells was evidential. (f) By removing cells from the PLGA-TCP composite it was observed that the thin layer of PLGA that coated the surfaces of some TCP particles was eroded.

ite was dramatically higher than on PLGA film and PLGA-HA composite ($p < 0.001$).

SEM observations

The original PLGA film surfaces were observed by SEM to be very smooth [Fig. 4(a)]. One week after seeding, RAW 264.7 cells proliferated and covered most of the available surface area of the PLGA film. Morphologically, RAW 264.7 cells could be seen as individual cells (6–10 μm diameter), groups of aggregated cells, and giant cells (20–30 μm diameter) as seen in Figure 4(c). However, there were no mature osteoclastic cells observed in any of the samples. By treatment with 10% Triton X100, the cells and any cellular fragments were detached from the material sur-

faces. There was a slight surface change caused by air drying; however, erosion of the PLGA surfaces was clearly evident [Fig. 4(e)]. The resorption lacunae formed by cells were between 5 and 30 μm , that is in the range of cell sizes observed.

In PLGA-TCP composite, TCP ceramic particles were evenly coated with a thin layer of PLGA film [Fig. 4(b)]. The morphology and sizes of RAW 264.7 cells on PLGA-TCP were similar to those on the surface of PLGA [Fig. 4(d)]. By detaching cells using Triton X100, it was observed that the thin layer of PLGA that coated the surfaces of some TCP particles was eroded. Some resorption lacunae were formed between TCP particles [Fig. 4(f)]. However, in the deep parts of the materials, the TCP particles were still embedded inside PLGA without erosion.

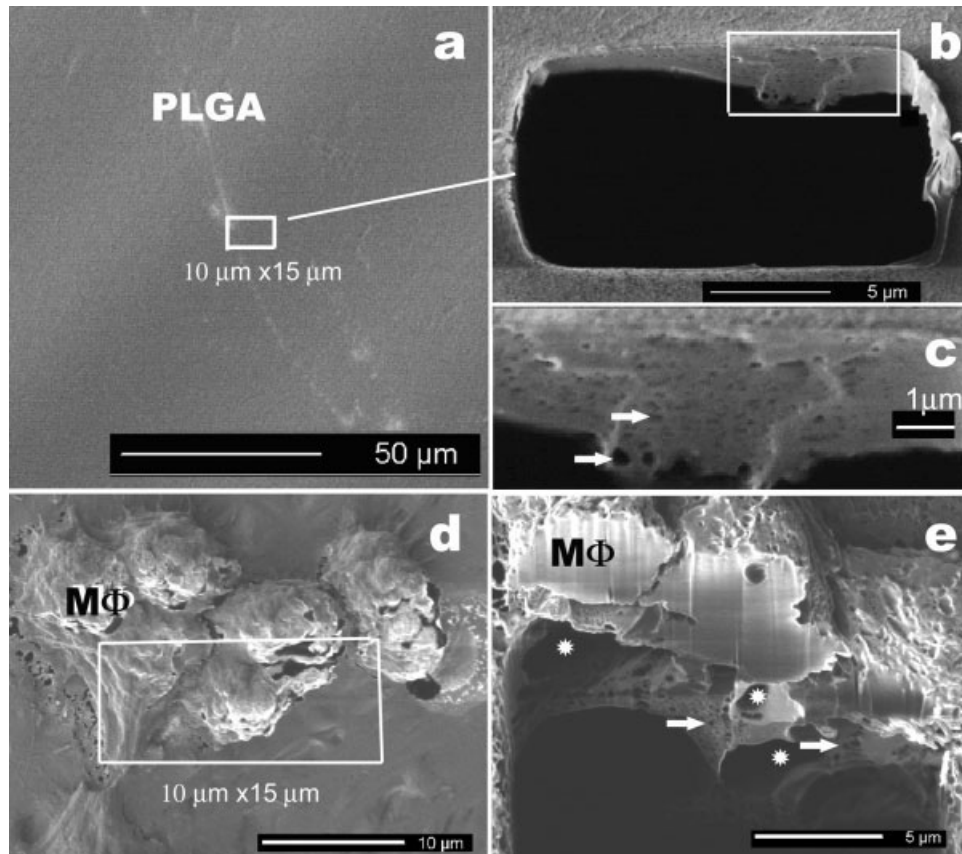


Figure 5. FIB-induced secondary electron images of (a) the control PLGA film with a smooth surface. (b) After milling, the PLGA film in the chosen area was removed. The cross-section was shown with the sample tilt of 45°. One area in a rectangle (inset) was chosen for high magnification as shown in (c) where many small pores in the film were visible as pointed by the arrows. (d) A group of RAW 264.7 cells (MΦ) on the PLGA film after 1 week's seeding. (e) The cross-section of cells on PLGA film after milling viewed at the sample tilt of 45°. The gap between cells showed that they are individual cells (MΦ). There were large pores formed in the film (some of them marked as stars, which were different from the small pores (pointed by the arrows) from the original film (c)).

FIB observations

Figure 5(a) shows the original film surface on the substrate of the control PLGA, which appears very smooth. The cross-section of the PLGA film in an area defined in Figure 5(a) was obtained by the FIB milling, as shown in Figure 5(b), an image taken in the FIB with the sample surface tilted at 45°. From Figure 5(c), the film was found to contain many nonconnected small pores, sized between 0.1 and 0.5 μm. After one week's seeding, RAW 264.7 cells were found to attach to the PLGA film surface and distributed as either individual cells with the size of $9.83 \pm 0.21 \mu\text{m}$ or as cell clusters [Fig. 5(d)]. There were gaps between the cells, and large resorption lacunae, which were different from the small pores in the film, formed at the interface between the cells and the film [Fig. 5(e)].

RAW 264.7 cells also formed MNGC [Fig. 6(a)]. The gaps between the individual cells were merged in MNGCs indicating cell fusion, although some trace of fusion was still evident [Fig. 6(b,c)]. Cross-sections of the interface between MNGC and PLGA

film demonstrated that the pseudopodia of MNGC deeply penetrated into PLGA film to form separated compartments. The PLGA film was eroded within the compartments and left resorption lacunae of approximately 1–10 μm size. Underneath the resorption lacunae, pores of sizes 0.1–0.5 μm diameter in the PLGA film were observed [Fig. 6(c)].

DISCUSSION

The mechanisms of PLGA degradation have been extensively studied. In general, the degradation is considered to be bulk erosion via hydrolysis,⁸ where the interior of the polymer is degraded first and disappears over a period of time, and the outer surface remains as a shell and is degraded later.¹⁰ This phenomenon is also observed on PLGA thin film degradation *in vitro*.²⁹ However, when RAW 264.7 cells, the murine macrophagic cell line, were used in the present study, the PLGA film was observed to be eroded from the surface within one week.

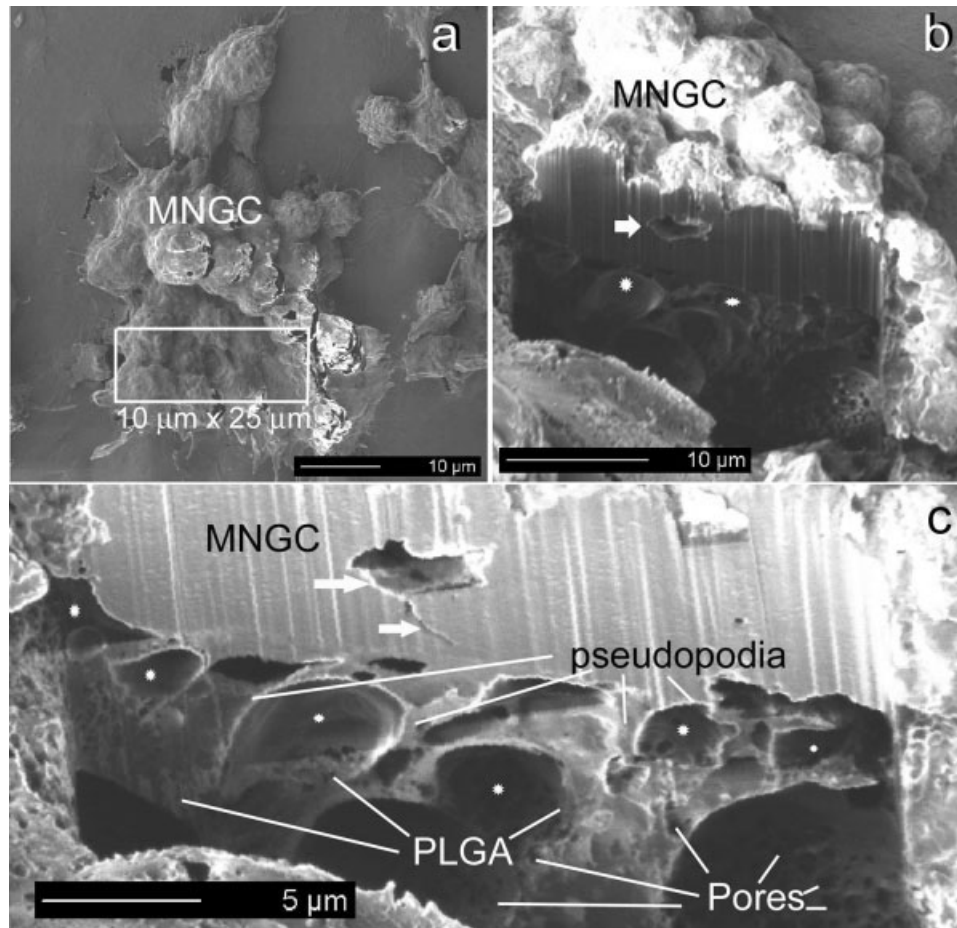


Figure 6. FIB induced secondary electron images showing the erosion of PLGA by the MNGC. (a) A MNGC formed from about 30 RAW 264.7 cells. A $10\ \mu\text{m} \times 25\ \mu\text{m}$ rectangle was selected on the MNGC for milling. (b) The cross-section of the interface between MNGC and PLGA film viewed with the sample tilted 45° after milling. (c) A high magnification of (b). There was a remaining gap within the MNGC (arrows). The pseudopodia of MNGC deeply penetrated into the PLGA film, resulting in the formation of the compartments (marked as stars). The PLGA film was eroded within the compartments and left as size 1–10 μm diameter resorption lacunae. Beneath the resorption lacunae, PLGA film contained pores with the size ranged from 0.1 to 0.5 μm was seen, which are identical with those seen in original porous film. The striations visible in (b) and (c) are FIB artefacts due to surface topography.

It has been reported that macrophages actively respond to polymeric materials both *in vitro* and *in vivo*. These responses include adhesion, proliferation, fusion to form MNGCs on polymeric materials,^{23,24} engulfment, and degradation materials.^{18,19,22,24}

To initiate the process of biodegradation, macrophages need first to attach to biomaterials. Although PLGA does not appear to be an ideal surface for fibroblastic cell adhesion, it does not affect macrophagic attachment. This may be due to the fact that macrophages express pattern recognition receptor and specific integrins that enable them to adhere to these surfaces. Cytoskeletal and adhesive structure studies of FBGC formation *in vitro* have demonstrated that podosomal structures, and not focal contacts, are the major adhesive structures present within macrophages and FBGCs on surfaces.^{30,31}

Not only can RAW 264.7 cells attach to PLGA surfaces, they also proliferate to increase in numbers af-

ter attachment and exhibit macrophage aggregation. Fusion of cells can be observed to form MNGCs. The mechanism controlling fusion of macrophages to form MNGCs is complex, although the macrophage mannose receptor has been identified as critical.^{32,33}

Via co-operation, groups of macrophages form MNGCs, or FBGCs, on PLGA surfaces. The consequences of the activities of macrophage and MNGCs or FBGCs activate the surface erosion of the PLGA film within the resorbing area. By detaching RAW 264.7 cells from the surface using Triton X100, the surface erosion seen in Figure 4(e–f) dramatically demonstrates the erosion processes on the surface of the PLGA.

Using FIB methods we have revealed the interface between MNGCs and PLGA biomaterials. By sealing an area of the polymers with pseudopodia on the cell surface, macrophages and MNGCs form separate compartments and erode polymers within the compartments.

The pseudopodia on the surface of MNGCs not only attach to the material surfaces but actually penetrate into the PLGA film. The fusion following cell adhesion may be an important step in initiation of biodegradation by increasing resorbing area and forming a sealing zone. It has been reported that phagocytosis via the formation of a closed compartment between the FBGCs and the underlying substrate into which degradative enzymes, reactive oxygen intermediates, and/or other products are secreted.¹¹ Thus, these secretions may play an important role in the extracellular erosion of PLGA.

The responses of macrophages and FBGCs to implantation of biomaterials are generally regarded as inflammatory reactions and widely treated as negative factors in biomaterial implantation. However, it is still unknown if blocking these cellular responses will benefit compatibility or inhibit degradation of biomaterials and subsequent tissue regeneration. As a secreting cell, the macrophage alone produces more than 100 cytokines, which play a critical role in cell activities, angiogenesis, and tissue regeneration in wound healing.¹³

It is well known that macrophages can differentiate into osteoclasts which can secrete protons for bone mineral resorption.^{14,15} However, there is no evidence for any osteoclast-like cell formation in the current study; whether the surface erosion of PLGA is due to enzymatic activity or local pH change is unknown. Further study is warranted to investigate the roles that macrophages and their fused MNGCs or FBGCs may play in bioerosion of polymeric biomaterials such as PLGA.

The valuable discussion with Professor David Cockyane is gratefully acknowledged.

References

- Gomes ME, Reis RL. Biodegradable polymers and composites in biomedical applications: From catgut to tissue engineering, Part 1. Available systems and their properties. *Inter Mater Rev* 2004;49:261–273.
- Athanasios KA, Niederauer GG, Agrawal CM. Sterilization, toxicity, biocompatibility and clinical applications of polylactic acid/polyglycolic acid copolymers. *Biomaterials* 1996;17:93–102.
- Okada H, Toguchi H. Biodegradable microspheres in drug delivery. *Crit Rev Ther Drug Carrier Syst* 1995;12:1–99.
- Guzman LA, Labhasetwar V, Song C, Jang Y, Lincoff AM, Levy R, Topol EJ. Local intraluminal infusion of biodegradable polymeric nanoparticles. A novel approach for prolonged drug delivery after balloon angioplasty. *Circulation* 1996;94:1441–1448.
- Eppley BL, Morales L, Wood R, Pensler J, Goldstein J, Havlik RJ, Habal M, Losken A, Williams JK, Burstein F, Rozzelle AA, Sadove AM. Resorbable PLLA-PGA plate and screw fixation in pediatric craniofacial surgery: Clinical experience in 1883 patients. *Plast Reconstr Surg* 2004;114:850–856; discussion 857.
- Kang SW, Jeon O, Kim BS. Poly(lactic-co-glycolic acid) microspheres as an injectable scaffold for cartilage tissue engineering. *Tissue Eng* 2005;11:438–447.
- Tamada JA, Langer R. Erosion kinetics of hydrolytically degradable polymers. *Proc Natl Acad Sci USA* 1993;90:552–556.
- von Burkersroda F, Schedl L, Gopferich A. Why degradable polymers undergo surface erosion or bulk erosion. *Biomaterials* 2002;23:4221–4231.
- Gopferich A. Mechanisms of polymer degradation and erosion. *Biomaterials* 1996;17:103–114.
- Li S, Garreau H, Vert M. Structure-property relationships in the case of the degradation of massive poly(α -hydroxy acid) in aqueous media, Part 1: poly (DL-lactic acid). *J Mater Sci Mater Med* 1990;1:123–130.
- Anderson JM, Shive MS. Biodegradation and biocompatibility of PLA and PLGA microspheres. *Adv Drug Deliv Rev* 1997;28:5–24.
- Lu L, Peter SJ, Lyman MD, Lai HL, Leite SM, Tamada JA, Uyama S, Vacanti JP, Langer R, Mikos AG. In vitro and in vivo degradation of porous poly(DL-lactic-co-glycolic acid) foams. *Biomaterials* 2000;21:1837–1845.
- Burke B, Lewis CE. *The Macrophage*. Oxford, UK: Oxford University Press; 2002.
- Teitelbaum SL. Bone resorption by osteoclasts. *Science* 2000; 289:1504–1508.
- Anderson JM. Multinucleated giant cells. *Curr Opin Hematol* 2000;7:40–47.
- Hickey T, Kreutzer D, Burgess DJ, Moussy F. In vivo evaluation of a dexamethasone/PLGA microsphere system designed to suppress the inflammatory tissue response to implantable medical devices. *J Biomed Mater Res* 2002;61:180–187.
- McKee MD, Nanci A. Secretion of Osteopontin by macrophages and its accumulation at tissue surfaces during wound healing in mineralized tissues: A potential requirement for macrophage adhesion and phagocytosis. *Anat Rec* 1996;245: 394–409.
- Lu J, Descamps M, Dejou J, Koubi G, Hardouin P, Lemaitre J, Proust JP. The biodegradation mechanism of calcium phosphate biomaterials in bone. *J Biomed Mater Res* 2002;63:408–412.
- Xia ZD, Zhu TB, Du JY, Zheng QX, Wang L, Li SP, Chang CY, Fang SY. Macrophages in degradation of collagen/hydroxylapatite(CHA), β -tricalcium phosphate ceramics (TCP) artificial bone graft. An in vivo study. *Chin Med J (Engl)* 1994;107:845–849.
- Lam KH, Schakenraad JM, Esselbrugge H, Feijen J, Nieuwenhuis P. The effect of phagocytosis of poly(L-lactic acid) fragments on cellular morphology and viability. *J Biomed Mater Res* 1993; 27:1569–1577.
- Solheim E, Sudmann B, Bang G, Sudmann E. Biocompatibility and effect on osteogenesis of poly(ortho ester) compared to poly(DL-lactic acid). *J Biomed Mater Res* 2000;49:257–263.
- Xia Z, Ye H, Choong C, Ferguson DJ, Platt N, Cui Z, Triffitt JT. Macrophagic response to human mesenchymal stem cell and poly(ϵ -caprolactone) implantation in nonobese diabetic/severe combined immunodeficient mice. *J Biomed Mater Res* 2004;71A:538–548.
- Brodbeck WG, Nakayama Y, Matsuda T, Colton E, Ziats NP, Anderson JM. Biomaterial surface chemistry dictates adherent monocyte/macrophage cytokine expression in vitro. *Cytokine* 2002;18:311–319.
- Chambers TJ, Spector WG. Inflammatory giant cells. *Immunobiology* 1982;161:283–289.
- Heimann RB, Wirth R. Formation and transformation of amorphous calcium phosphates on titanium alloy surfaces during atmospheric plasma spraying and their subsequent in vitro performance. *Biomaterials* 2005;27:823–831.
- Giannuzzi LA, Drown JL, Brown SR, Irwin RB, Stevie FA. Applications of the FIB lift-out technique for TEM specimen preparation. *Microsc Res Tech* 1998;41:285–290.

27. Ngo H, Cairney J, Munroe P, Vargas M, Mount G. Focused ion beam in dental research. *Am J Dent* 2000;13(Spec No): 31D–34D.
28. Itonaga I, Sabokbar A, Sun SG, Kudo O, Danks L, Ferguson D, Fujikawa Y, Athanasou NA. Transforming growth factor- β induces osteoclast formation in the absence of RANKL. *Bone* 2004;34:57–64.
29. Lu L, Garcia CA, Mikos AG. In vitro degradation of thin poly (DL-lactic-co-glycolic acid) films. *J Biomed Mater Res* 1999;46:236–244.
30. DeFife KM, Jenney CR, Colton E, Anderson JM. Disruption of filamentous actin inhibits human macrophage fusion. *FASEB J* 1999;13:823–832.
31. DeFife KM, Jenney CR, Colton E, Anderson JM. Cytoskeletal and adhesive structural polarizations accompany IL-13-induced human macrophage fusion. *J Histochem Cytochem* 1999;47:65–74.
32. DeFife KM, Jenney CR, McNally AK, Colton E, Anderson JM. Interleukin-13 induces human monocyte/macrophage fusion and macrophage mannose receptor expression. *J Immunol* 1997;158:3385–3390.
33. Dadsetan M, Jones JA, Hiltner A, Anderson JM. Surface chemistry mediates adhesive structure, cytoskeletal organization, and fusion of macrophages. *J Biomed Mater Res A* 2004; 71:439–448.